



## Fabrication and mechanical properties of bulk NiTi/Al composites prepared by friction stir processing



D.R. Ni<sup>a</sup>, J.J. Wang<sup>a,b</sup>, Z.N. Zhou<sup>b</sup>, Z.Y. Ma<sup>a,\*</sup>

<sup>a</sup>Shenyang National Laboratory for Materials Science, Institute of Metal Research, Chinese Academy of Sciences, 72 Wenhua Road, Shenyang 110016, China

<sup>b</sup>School of Materials Science and Engineering, Shenyang Aerospace University, Shenyang 110136, China

### ARTICLE INFO

#### Article history:

Received 21 August 2013

Received in revised form 20 September 2013

Accepted 2 October 2013

Available online 14 October 2013

#### Keywords:

Friction stir processing

Shape memory alloy

Metal matrix composites

Microstructure

Mechanical properties

### ABSTRACT

Friction stir processing (FSP) was used to prepare NiTi reinforced 6061Al bulk composites with the aim to avoid deleterious Al–NiTi interface reaction occurred in cast and powder metallurgy processes. NiTi were homogeneously distributed in the Al matrix without interfacial reaction. The intrinsic characteristic of a reversible thermoelastic phase transformation of the NiTi was observed in the composites. The as-FSP composites showed lower tensile strengths and higher elongation than the as-received 6061Al–T651, and the strengths increased greatly after both aging and T6 heat treatments without interfacial products being detected. The results show that FSP is an effective way to produce NiTi/Al composites with good shape memory effect and mechanical properties.

© 2013 Elsevier B.V. All rights reserved.

### 1. Introduction

Shape memory alloys (SMAs) have the ability to recover their original shape after deformation resulting from stress and temperature induced transformations between austenitic and martensitic phases. This phenomenon is known as shape memory effect (SME) [1–3]. It is promising to introduce the SMAs into light alloys to prepare special metal matrix composites (MMCs) with a low density, high strength, and moderate SME.

However, previous investigations showed that it is not desirable to fabricate SMAs reinforced MMCs using common cast and powder metallurgy (PM) processes, because the serious interfacial reaction and interfacial diffusion occurred between the SMAs and the matrix alloys at high temperatures [4–6]. This leads to the formation of intermetallics which are injurious to the interfacial bonding strength and degrade the SME due to the variation in the composition of the SMAs [7,8]. Therefore, avoiding the occurrence of interfacial reaction and interfacial diffusion is the key to fabricate SMAs reinforced MMCs.

Friction stir processing (FSP) is a solid-state processing technique developed based on the basic principles of friction stir welding (FSW) [9,10]. FSP can be adopted to fabricate MMCs, especially those difficult to produce by conventional methods. Mishra et al. [11] first reported the FSP fabrication of a surface SiCp/Al layer 50–200 μm in thickness. Since then, FSP has been widely applied

in producing various kinds of MMCs. FSP fabrication of MMCs can be divided into two kinds, the indirect FSP method and the direct FSP method. In the indirect FSP method, particles are pre-mixed with the matrix powders and cold compacted and/or hot pressed to form a bulk billet, and then subjected to FSP to form the final composites [12–16]. In the direct FSP method, the particles are firstly preset on the surface or into the grooves or holes of a plate and then subjected to FSP, incorporating the particles directly into the matrix materials.

So far, the direct FSP method has been used to prepare various magnesium and aluminum matrix composites and the reinforcements adopted include SiO<sub>2</sub>, C60, carbon nanotube, Al<sub>2</sub>O<sub>3</sub>, and SiC, etc. [17–21]. While the direct FSP method is simple, quick, and economical, it is difficult to obtain composites with homogeneously distributed particles. Furthermore, this method was mainly concentrated on surface composites, and how to obtain bulk composites is still a great challenge. The presetting method of particles is a key controlling factor in obtaining composites with good properties. Now, the widely adopted presetting method is to cut a groove on the surface of a plate and put particles into it. In some cases, a thin plate is used as a lip to cover the groove [21]. However, during FSP the particles in the groove are likely to be pushed forward by the rotating tool, resulting in the agglomeration and loss of particles.

Recently Dixit et al. [22] reported the fabrication of a NiTi/1100Al surface composite by FSP. In their study, the NiTi were preset into four holes, 1.6 mm in diameter and 76 mm in length, drilled at about 0.9 mm below the plate surface and parallel to the

\* Corresponding author. Tel./fax: +86 24 83978908.

E-mail address: [zyrna@imr.ac.cn](mailto:zyrna@imr.ac.cn) (Z.Y. Ma).

surface. After FSP, no interfacial reaction occurred around the NiTiP. The SME of the NiTiP could induce residual compressive and tensile stresses in the matrix, improving the mechanical properties of the composite [22]. This indicates that the SMAs reinforced MMCs with a good interfacial bonding could be prepared by FSP. However, in order to achieve a wide application of the SMAs reinforced MMCs as smart materials for making sensors or actuators, it is necessary to fabricate the bulk composites to understand their physical and mechanical properties associated with the SME.

In this study, the feasibility of preparing bulk NiTiP/6061Al composites by the direct FSP method was investigated. A special multi-hole particle presetting mode was adopted, which could help to homogeneously distribute the particles in the matrix. The tensile properties and fracture behavior of the composite under different heat-treatment conditions were carefully examined.

## 2. Materials and methods

Commercial 6061Al–T651 rolled plates (T6: Solution-treated and then artificially aged; T651: Solution-treated, stress relieved by stretching, and then artificially aged), with a nominal composition of Al–1.0Mg–0.6Si–0.7Fe–0.4Cu–0.35Cr–0.4Mn–0.15Ti (wt.%), were used in this study. This alloy was chosen due to its good comprehensive mechanical properties and workability. Atomized Ni<sub>49.5</sub>Ti<sub>50.5</sub> (at.%) particles with two size ranges of 150–178 μm and 2–74 μm (hereafter referred to as large and small particles) were adopted, respectively, and most of the NiTiP exhibited spherical structures (Fig. 1).

Fig. 2 shows the schematic diagram of preparing the bulk NiTiP/6061Al composites by FSP. A series of holes 4 mm in diameter and 5 mm in depth were machined on the plates with dimensions of 200 × 70 × 6 mm perpendicular to the plate surface. The wall thickness between adjacent holes was about 0.5–1.0 mm. The NiTiP were embedded in the holes and compacted at about 5 MPa. A four-pass FSP, with a 100% overlap and the same forward directions, was conducted to the NiTiP filled plates at a tool rotation rate of 600 rpm and a traversing speed of 100 mm min<sup>-1</sup>. A M42 steel tool with a shoulder 24 mm in diameter and a threaded cylindrical pin 8 mm in diameter and 4.8 mm in length was used. The tilt angle of the tool was 2.7° and the plunged depth was controlled to be about 0.2 mm for each FSP pass. To understand the effect of heat treatment on the microstructures and mechanical properties of the composites, the as-FSP composite was subjected to a T6 heat treatment: solution treated at 515 °C for 40 min, 25 °C water quenched, and then aged at 163 °C for 18 h. For comparison, a matrix plate was subjected to FSP and T6 heat treatment under the same condition.

The composite reinforced with the large NiTiP was subjected to differential scanning calorimetry (DSC) analyses on a DSC Q1000 V9.4 Build 287 machine. The test was conducted over a temperature range of –60–110 °C at a rate of 10 °C min<sup>-1</sup>. The adopted temperature range would be suitable for the DSC testing of the NiTiP and NiTiP/6061Al composites according to previous reports [4,22]. For comparison, the NiTiP were cold compacted into a billet of similar dimensions and subjected to DSC at the same condition.

The microstructures of the composites were examined using scanning electron microscopy (SEM) coupled with an energy-dispersive X-ray spectroscopy (EDS), transmission electron microscopy (TEM), and high resolution electron microscopy (HRTEM). The SEM specimens were cross-sectioned perpendicular to the FSP direction and polished without etching. Thin foils for TEM and HRTEM were prepared by ion thinning. Sub-sized tensile specimens with a gauge section of 5 × 1.5 × 0.85 mm were machined parallel to the FSP direction. Tensile tests were conducted at a strain

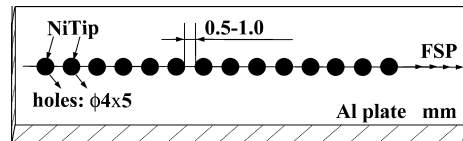


Fig. 2. Schematic diagram of preparing bulk NiTiP/6061Al composites by FSP.

rate of  $1 \times 10^{-3} \text{ s}^{-1}$  at room temperature using an Instron 5848 tensile tester. The total elongation of samples was calculated by measuring the breaking length of the tensile specimens. The property data for each condition were obtained by averaging 3 test results. The tensile fracture surfaces were examined by SEM.

## 3. Results

### 3.1. Microstructure

The NiTiP/6061Al composites had a thickness of about 5 mm, which was much thicker than the surface composite (~2 mm) in Ref. [22]. The volume fraction of the NiTiP in both the composites was estimated to about 10% by using an image analysis software. SEM examinations revealed two important findings (Fig. 3a and b). First, the NiTiP were homogeneously distributed in the Al matrix with the small NiTiP exhibiting more homogeneous distribution, and only a few NiTiP were found to be slightly damaged. Second, the interface between the NiTiP and the Al matrix was clean without discernible reaction products, and this was also verified by the backscattered electron image (BSE) and EDS line scan analyses (Fig. 3c). TEM examinations further confirmed that no interfacial reaction occurred (Fig. 3d). These indicate that the bulk composites reinforced by homogeneously distributed NiTiP were successfully prepared. The SEM observation of the microstructures showed that after a T6 heat treatment the interface was clean and no reaction products were detected (Fig. 4a). The TEM and HRTEM examinations further confirmed that the interface between the NiTiP and the Al matrix was clean and no interfacial products existed (Fig. 4b and c).

### 3.2. Shape memory effect

The DSC results showed that the composite and the as-received NiTiP exhibited a similar phase transformation behavior during the heating and cooling cycles (Fig. 5). An endothermic peak appears on the heating curve of each sample, which corresponds to the martensite to austenite transformation. Two peaks are visible on the cooling curve of the as-received NiTiP: the first peak is weak and relates to the austenite to R-phase transformation; the second peak is strong and relates to the R-phase to martensite

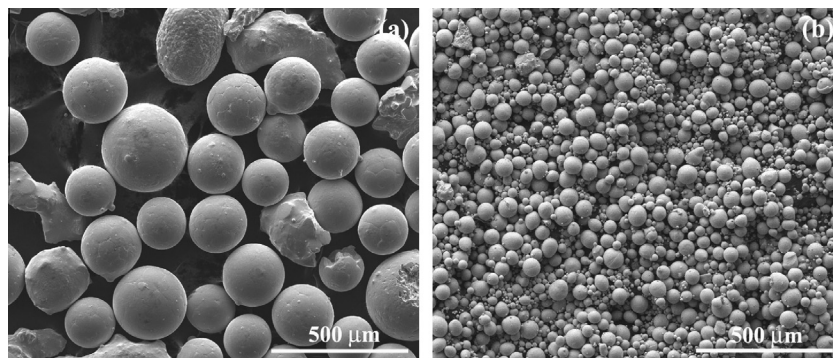
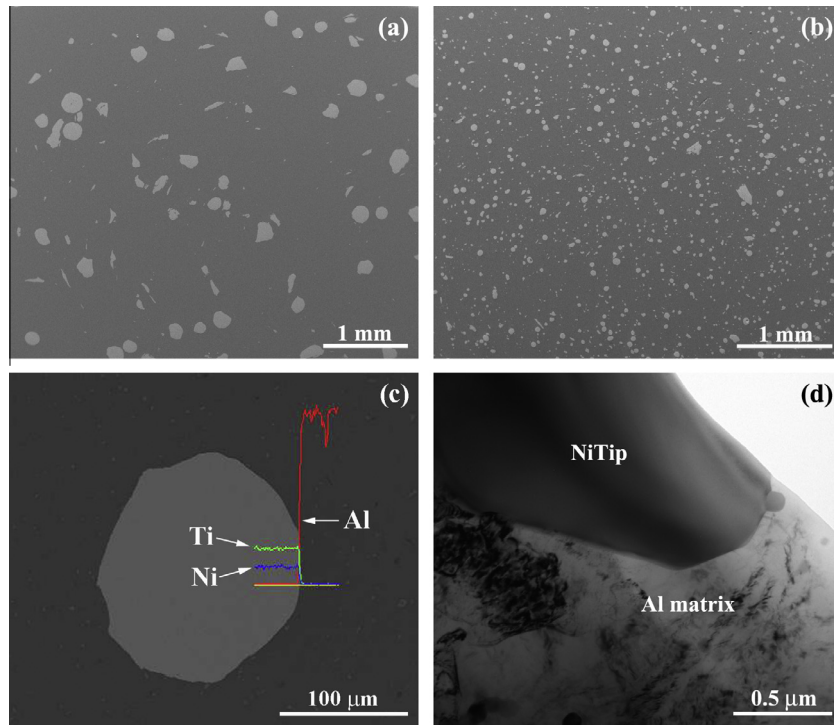
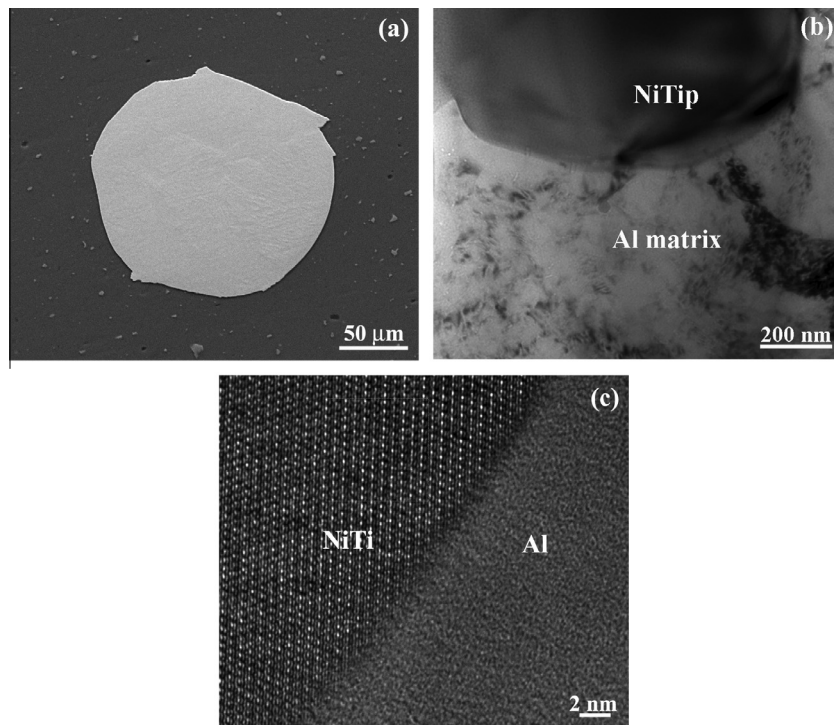


Fig. 1. Morphologies of as-received NiTiP with sizes of (a) 150–178 μm and (b) 2–74 μm.



**Fig. 3.** SEM images showing uniform distribution of NiTi in (a) large and (b) small NiTi reinforced 6061Al composite, (c) backscattered electron image (BSE) and EDS line scan showing no interfacial reaction, and (d) TEM image showing no interfacial reaction.



**Fig. 4.** Microstructure of large NiTi reinforced 6061Al composite after T6 heat treatment showing no interfacial reaction: (a) SEM, (b) TEM, and (c) HRTEM.

transformation. However, only the austenite to martensite transformation peak is visible on the cooling curve of the composite, and the composite showed narrower transformation ranges compared to the as-received NiTi.

### 3.3. Tensile properties and fractography

The results of tensile properties of the 6061Al and NiTi/6061Al composites reveal the following observations (Table 1). First, while

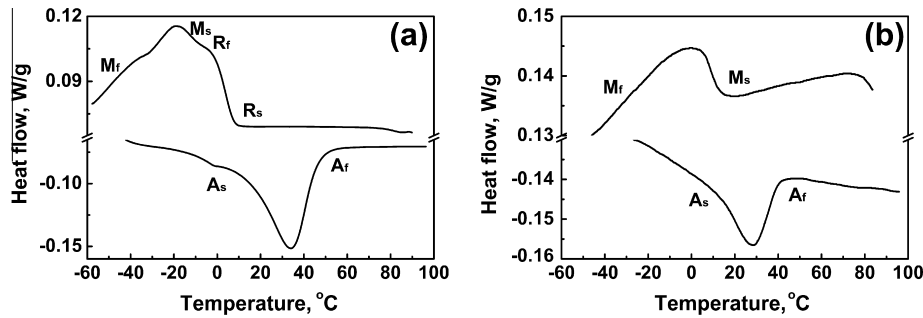


Fig. 5. DSC curves of (a) as-received NiTip and (b) large NiTip reinforced 6061Al composite.

**Table 1**  
Tensile properties of 6061Al and NiTip reinforced 6061Al composites.

Sample		UTS, MPa	YS, MP	EL, %
6061Al	BM	330 ± 5	292 ± 5	14.4 ± 2.6
	BM-T6	323 ± 4	296 ± 3	12.4 ± 1.1
	FSP	275 ± 8	156 ± 8	26.2 ± 1.6
	Aging-treated	345 ± 4	281 ± 3	19.7 ± 0.6
	T6-treated	368 ± 3	332 ± 5	16.6 ± 2.0
Large NiTip/6061Al	FSP	220 ± 3	116 ± 2	20.4 ± 1.5
	Aging-treated	318 ± 19	281 ± 8	7.0 ± 1.8
	T6-treated	317 ± 6	267 ± 4	8.8 ± 0.6
Small NiTip/6061Al	FSP	247 ± 8	134 ± 5	18.4 ± 3.2
	Aging-treated	350 ± 9	304 ± 2	9.1 ± 0.6
	T6-treated	341 ± 10	308 ± 9	7.8 ± 3.3

the as-received T651 base metal (BM) showed a good combination of strength and ductility, the T6 treatment slightly decreased the tensile properties. Second, the as-FSP 6061Al showed lower strengths than the as-received T651 BM, whereas both the aging-treated and T6-treated FSP 6061Al, especially the latter exhibited a significant enhancement in strengths and ductility. Third, both the as-FSP and T6-treated composites exhibited lower strengths and ductility compared to their counterparts of the 6061Al, respectively. Fourth, under the aging-treatment condition, the composites reinforced by the large and small particles showed strengths similar to and better than, respectively, their counterparts of the 6061Al, but with lower ductility. Fifth, the composite reinforced by the small NiTip showed higher YS and UTS than that reinforced by the large NiTip under the as-FSP, aging, and T6-treatment conditions, but their elongations were at the same level. Sixth, although the T6-treated FSP 6061Al showed higher strengths than the aging-treated 6061Al, the T6 and aging treatments showed similar effects to the as-FSP composites in increasing the strength and decreasing the ductility.

Fig. 6 shows the SEM fractographs of the BM and the composite reinforced by the small NiTip under the as-FSP, aging, and T6-treatment conditions. The fracture surface of the BM was covered with many dimples and showed typical features of ductile fracture (Fig. 6a). By comparison, the fracture surface of the as-FSP composite was characterized by the pull-out of NiTip and the fine dimples with reduced number and size (Fig. 6b). However, the NiTip were generally covered with the Al matrix. At a high magnification, it was clear that the surfaces of the NiTip were fully covered with the Al dimples (Fig. 6c). Furthermore, it was found that the bottoms of the pits resulting from the pullout of NiTip were also covered with the Al dimples (Region C in Fig. 6b). In the case of the T6-treated composite (Fig. 6d), the dimples were much shallower than those in the as-FSP composite. Meanwhile, the Al dimples on the NiTip surfaces were also less (Fig. 6e). EDS results (Table 2) reveal that the surfaces of the pulled-out NiTip contained

Ti, Ni, Al, Si, and Mg elements, showing that it was covered with a layer of 6061Al matrix (Regions A and B in Fig. 6b). No Ni or Ti element was found at the bottoms of the pits (Region C in Fig. 6b). After the T6-treatment, the Al content on the surfaces of the pulled-out NiTip decreased (Regions D and E in Fig. 6d). For the aging-treated composite, the morphology of the fracture surface was somewhat similar to that of the T6-treated composite (Fig. 6f).

Fig. 7a and b shows the SEM fractographs of the composite reinforced by the large NiTip under the as-FSP and T6-treatment conditions, respectively. Similar to that of the composite reinforced by the small NiTip, the pulled-out NiTip and pits covered with dimples were found on the fracture surface of the as-FSP composite. After the T6-treatment, the dimples on the surfaces of NiTip became indistinct.

## 4. Discussion

### 4.1. Microstructures

As described above, for the direct FSP method of producing the composites, the main difficulty is achieving a homogeneous distribution of particles, and therefore the particle presetting mode is a key factor. For the multi-hole presetting mode in this study, the walls between adjacent holes could effectively prevent the particles from being pushed forward or out by the rotating tool, thereby avoiding the agglomeration and loss of the particles. Furthermore, such a particle presetting mode is beneficial to the precise control of the particle content in the fabricated composites. This indicates that the multi-hole presetting mode has a function of achieving particle pre-distribution, and provides an efficient way to produce the bulk composites.

The NiTip reacted easily with Al at high temperatures, resulting in the generation of intermetallics on the NiTi–Al interface [4,5], which was harmful to the interfacial bonding strength [7,8]. Recently, Thorat et al. [6] investigated the transformation behavior of the NiTip/2124Al prepared by the PM process (sintered at 500 °C for 90 min, then hot extruded at 480 °C). The interface reaction between the NiTip and Al was obvious, and the NiTip were surrounded by a layer of diffused interface products, Al<sub>3</sub>Ti and Al<sub>3</sub>Ni; meanwhile, Al atoms diffused into the NiTip to form an Al-rich layer. The presence of Al lowered the Ni concentration of NiTip, and this affected the transformation behavior by broadening the intermediate R-phase transformation range. More recently, San Martín et al. [23] modified the process by shortening the sintering time from 90 to 15 min and decreasing the extrusion temperature from 480 to 430–440 °C, and reported that no intermetallics were observed at the interface. However, for the PM process, the considerably shortened sintering time and lower temperature are not beneficial to the diffusion and bonding between the powders, and the densification of the billets, especially for the preparation of large billets.

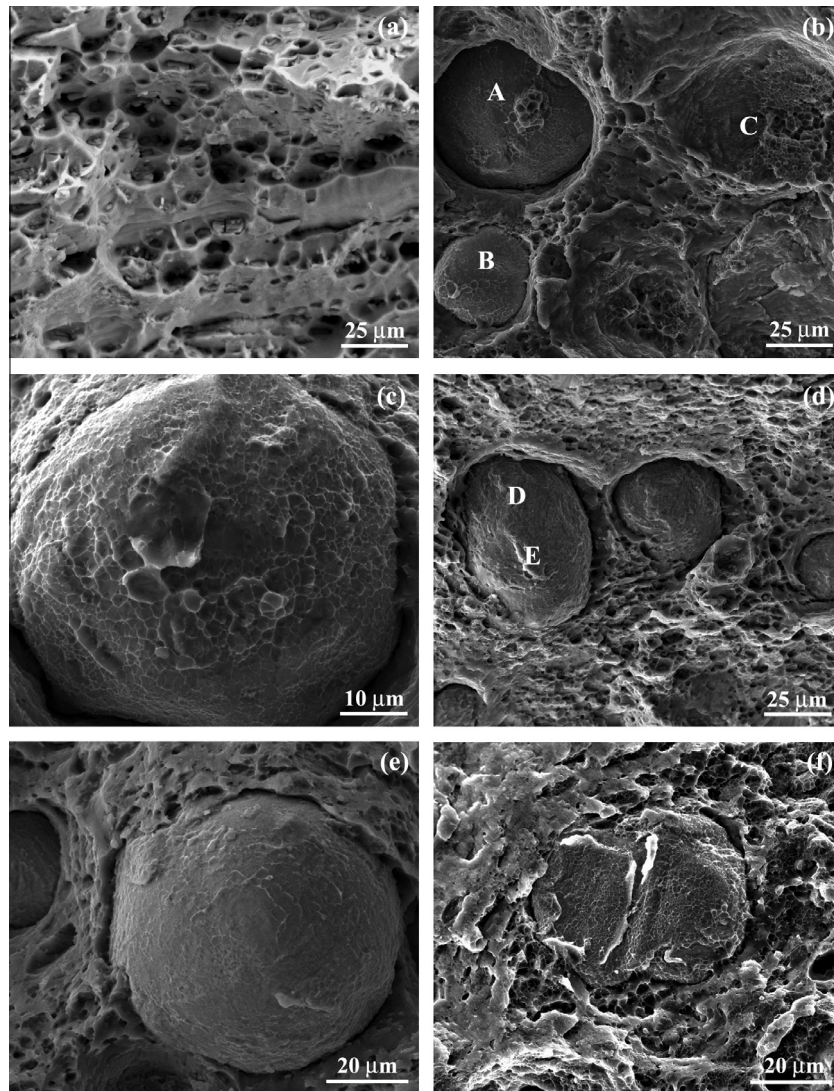


**Fig. 6.** SEM fractographs of as-received 6061Al and small NiTi reinforced 6061Al composite: (a) BM, (b) as-FSP composite, (c) a pulled-out NiTi in as-FSP composite, (d) T6-treated composite, (e) a pulled-out NiTi in T6-treated composite, and (f) aging-treated composite.

**Table 2**  
Results of EDS analysis of Fig. 7 (weight percent).

Region	Ti	Ni	Al	Si	Mg
A	29.5	33.5	36.0	0.9	–
B	33.5	37.3	26.7	1.5	1.0
C	–	–	100.0	–	–
D	44.1	50.0	3.4	2.5	–
E	39.5	38.6	15.8	5.0	1.1

As discussed above, how to control the interfacial reaction between the NiTi and the Al matrix is the most important challenge for producing the NiTi/Al composites. For the as-FSP composites, the interfacial reaction was completely inhibited (Fig. 3). This is attributed to the following two factors. First, the duration of the FSP process was significantly shorter than that of the PM process: the thermal exposure to higher temperatures lasted only about several seconds and the whole FSP process lasted only about several minutes [24]. Second and most important, the temperature during FSP was much lower than that during the PM process. For example, the maximum temperature in the nugget during FSW of 6063Al was about only 400 °C at a rotation rate of 800 rpm [24].

The microstructures of the T6-treated composites showed that the interface between the NiTi and the Al matrix was clean without discernible interfacial products, indicating that the NiTi were stable in the Al matrix at a high temperature up to 515 °C after 40 min. This means that the as-FSP composite could be strengthened through the conventional T6-treatment, and this will be further discussed later.

#### 4.2. Shape memory effect

The DSC results indicated that the NiTi/6061Al composite showed the phase transformation effect of the as-received NiTi (Fig. 5). For the NiTi alloy, the R-phase usually appears before the formation of martensite during cooling. Thus there were two peaks on the cooling curve of the as-received NiTi: the austenite to R-phase and the R-phase to martensite transformation peaks. However, in the case of the NiTi/6061Al composite, only the austenite to martensite transformation peak appeared on the cooling curve. This indicates that the FSP procedure might change the phase transformation behavior of the NiTi, but another more possible reason is that the lower content of NiTi in the composite made the peak undistinguished in the DSC curve. The present

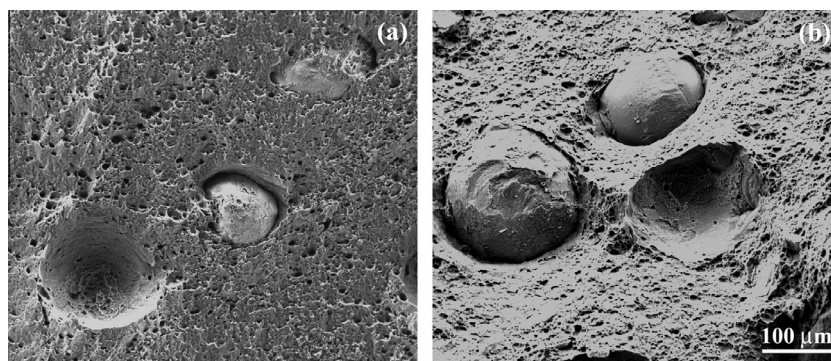


Fig. 7. SEM fractographs of large NiTip reinforced 6061Al composite: (a) as-FSP, and (b) T6-treated.

study shows that besides the intrinsic characteristic – one-way SME, this composite can also exhibit a two-way SME which is an acquired characteristic and can be obtained by training. Detailed investigation of physical properties of this composite will be presented elsewhere.

#### 4.3. Tensile properties and fractography

Compared to the as-received T651 BM with good strength and moderate ductility, the as-FSP 6061Al exhibited much lower tensile strength and higher ductility. This is ascribed to the microstructure change due to high temperature exposure and dynamic recrystallization during FSP. Our previous investigations [25–27] on the FSW of 6061Al–T651 showed that a high density of fine needle-shaped primary  $\beta''$  ( $\text{Mg}_2\text{Si}$ ) strengthening precipitates were observed in the BM, but no  $\beta''$  were detected after FSW, showing that FSW resulted in the dissolution of the  $\beta''$ . Despite a strong solid solution strengthening and smaller grain size, the nugget zone was softer than the BM. Clearly, the variation in the strength of 6061Al after FSP in this study is consistent with the previous reports [25–27]. The T6-treatment increased the strengths of the FSP 6061Al because of the precipitation of the fine  $\beta''$  particles [28,29]. However, the T6-treated 6061Al showed higher strengths and elongation than the as-received T651 BM, and this should be ascribed to the finer grain sizes in the FSP 6061Al resulting from the dynamic recrystallization during FSP. When the as-received T651 BM was subjected to a T6-treatment, both the UTS and elongation decreased slightly with the YS changed little, this is attributed to the disappearance of the work hardening effect. Furthermore, it was noticed that the aging-treated FSP 6061Al also showed a good combination of strength and ductility, showing that the FSP process can play the role of the solid solution treatment.

For the as-FSP composites, despite the existence of NiTip, the soft 6061Al matrix made the composites exhibit lower strengths but higher ductility than the as-received T651 BM. Both the aging and T6 treatments increased the strengths of the as-FSP composites because the soft matrix was strengthened. The relatively large size of the NiTip should be responsible for the lower strengths and ductility of the composites compared to those of the 6061Al matrices under the as-FSP and T6-treatment conditions. It is well documented that large sized particles generally did not show a desired strengthening effect on the metal matrix, and this has been systematically analyzed and widely verified in the SiCp/Al composites [30–32]. Likewise, this also explains why the large NiTip reinforced composite showed lower tensile strengths than that reinforced by the small NiTip.

It is noted that both the T6-treated and aging-treated composites reinforced by the small NiTip exhibited an extremely high UTS equivalent to that of a T6-treated 6082Al composite reinforced by

22.9 vol.% NiTi fiber [33]. However, previous investigations [34,35] showed that the heat treatments like aging at 300–600 °C could result in the precipitation of fine  $\text{Ni}_4\text{Ti}_3$  particles and change the density and distribution of dislocations within NiTi alloys, which may result in the slight change of the shape memory behavior. This means that the T6 heat treatment might change the SME of the composites, and this will be further investigated in our future study.

The fracture surface of the as-FSP composite (Fig. 6b) showed less dimples with a smaller size compared to that of the BM (Fig. 6a). This is attributed to its fine and equiaxed recrystallized grain structure. The Al dimples on the NiTip surfaces (Fig. 6c, e, and f) showed that a good interfacial bonding strength existed between the NiTip and the Al matrix. The EDS results further revealed that no interfacial debonding occurred (Table 2). The fracture appeared within the matrix near the NiTip. Although some pits were found due to the pullout of the NiTip (Figs. 6b and 7a), the Al dimples at their bottoms indicated that the bonding between the NiTip and the Al matrix was in good condition. The T6-treated composite showed shallower and indistinct dimples (Figs. 6d and 7b), and this may be responsible for its lower ductility.

## 5. Conclusions

In summary, the following conclusions are reached:

1. Bulk NiTip/6061Al composites were successfully prepared by FSP using a novel multi-hole particle presetting mode, which could effectively prevent the agglomeration and loss of particles. The NiTip were homogeneously distributed in the Al matrix without discernible interfacial products. After the T6-treatment, no reaction products were found on the interface.
2. The composite exhibited a phase transformation behavior similar to that of the as-received NiTip.
3. The composite reinforced by the small NiTip showed higher strength than that by the large NiTip. The aging treatment provided a comparable strengthening effect with that of the T6-treatment on the as-FSP composite. The strengths of both the aging-treated and T6-treated composites reinforced by small particles were higher than those of the as-received T651 BM.
4. The SEM fractographs showed that the bonding between the NiTip and the Al matrix was good without interfacial debonding under both the as-FSP and T6-treatment conditions.

## Acknowledgements

This work was supported by the National Natural Science Foundation of China under Grant Nos. 51101155 and 51331008 and the

National Basic Research Program of China under Grant No. 2012CB619600.

## References

- [1] Y. Freed, J. Aboudi, Micromechanical prediction of the two-way shape memory effect in shape memory alloy composites, *Int. J. Solids Struct.* 46 (2009) 1634–1647.
- [2] W. Huang, On the selection of shape memory alloys for actuators, *Mater. Des.* 23 (2002) 11–19.
- [3] W. Cai, X.L. Meng, L.C. Zhao, Recent development of TiNi-based shape memory alloys, *Curr. Opin. Solid State M.* 9 (2005) 296–302.
- [4] G.A. Porter, P.K. Liaw, T.N. Tieg, K.H. Wu, Ni–Ti SMA-reinforced Al composites, *JOM* (2000) 52–56.
- [5] J.H. Lee, K. Hamada, K. Mizuuchi, M. Taya, K. Inoue, Microstructures and mechanical properties of 6061Al matrix smart composite containing TiNi shape memory fiber, *Mater. Res. Soc. Symp.* 459 (1997) 419–424.
- [6] R.R. Thorat, D.D. Risanti, D. San Martín, G. Garces, P.E.J. Rivera Díaz del Castillo, S. van der Zwaag, On the transformation behaviour of NiTi particulate reinforced AA2124 composites, *J. Alloys Comp.* 477 (2009) 307–315.
- [7] K. Mizuuchi, The fabrication and thermomechanical behavior of Al and Ti SMA composites, *JOM* (2000) 26–31.
- [8] Z.C. Wei, C.Y. Tang, W.B. Lee, Design and fabrication of intelligent composites based on shape memory alloys, *J. Mater. Process. Technol.* 69 (1997) 68–74.
- [9] Z.Y. Ma, Friction stir processing technology: a review, *Metall. Mater. Trans. A* 39A (2008) 642–658.
- [10] R.S. Mishra, Z.Y. Ma, Friction stir welding and processing, *Mater. Sci. Eng. R* 50 (2005) 1–78.
- [11] R.S. Mishra, Z.Y. Ma, I. Charit, Friction stir processing: a novel technique for fabrication of surface composite, *Mater. Sci. Eng. A* 341 (2003) 307–310.
- [12] C.J. Hsu, C.Y. Chang, P.W. Kao, N.J. Ho, C.P. Chang, Al–Al<sub>3</sub>Ti nanocomposites produced in situ by friction stir processing, *Acta Mater.* 54 (2006) 5241–5249.
- [13] I.S. Lee, P.W. Kao, N.J. Ho, Microstructure and mechanical properties of Al–Fe in situ nanocomposite produced by friction stir processing, *Intermetallics* 16 (2008) 1104–1108.
- [14] C.M. Hu, C.M. Lai, X.H. Du, N.J. Ho, J.C. Huang, Enhanced tensile plasticity in ultrafine-grained metallic composite fabricated by friction stir process, *Scripta Mater.* 59 (2008) 1163–1166.
- [15] Z.Y. Liu, B.L. Xiao, W.G. Wang, Z.Y. Ma, Singly dispersed carbon nanotube/aluminum composites fabricated by powder metallurgy combined with friction stir processing, *Carbon* 50 (2012) 1843–1852.
- [16] Z.Y. Liu, B.L. Xiao, W.G. Wang, Z.Y. Ma, Elevated temperature tensile properties and thermal expansion of CNT/2009Al composites, *Compos. Sci. Technol.* 72 (2012) 1826–1833.
- [17] C.J. Lee, J.C. Huang, P.J. Hsieh, Mg based nano-composites fabricated by friction stir processing, *Scripta Mater.* 54 (2006) 1415–1420.
- [18] Y. Morisada, H. Fujii, T. Nagaoka, M. Fukusumi, Nanocrystallized magnesium alloy uniform dispersion of C60 molecules, *Scripta Mater.* 55 (2006) 1067–1070.
- [19] L.B. Johannes, L.L. Yowell, E.S.S. Arepalli, R.S. Mishra, Survivability of single-walled carbon nanotubes during friction stir processing, *Nanotechnology* 17 (2006) 3081–3084.
- [20] A. Shafiei-Zarghani, S.F. Kashani-Bozorg, A. Zarei-Hanzaki, Microstructures and mechanical properties of Al/Al<sub>2</sub>O<sub>3</sub> surfacenanocomposite layer produced by friction stir processing, *Mater. Sci. Eng. A* 500 (2009) 84–91.
- [21] E.R.I. Mahmoud, K. Ikeuchi, M. Takahashi, Fabrication of SiC particle reinforced composite on aluminium surface by friction stir processing, *Sci. Technol. Weld. Joining* 13 (2008) 607–618.
- [22] M. Dixit, J.W. Newkirk, R.S. Mishra, Properties of friction stir-processed Al 1100–NiTi composite, *Scripta Mater.* 56 (2007) 541–544.
- [23] D. San Martín, D.D. Risanti, G. Garces, P.E.J. Rivera Díaz del Castillo, S. van der Zwaag, On the production and properties of novel particulate NiTi/AA2124 metal matrix composites, *Mater. Sci. Eng. A* 526 (2009) 250–252.
- [24] Y.S. Sato, M. Urata, H. Kokawa, Parameters controlling microstructure and hardness during friction-stir welding of precipitation-hardenable aluminum alloy 6063, *Metall. Mater. Trans. A* 33A (2002) 625–635.
- [25] F.C. Liu, Z.Y. Ma, Influence of tool dimension and welding parameters on microstructure and mechanical properties of friction-stir-welded 6061–T651 Al alloy, *Metall. Mater. Trans. A* 39 (2008) 2378–2388.
- [26] A.H. Feng, D.L. Chen, Z.Y. Ma, Effect of welding parameters on microstructure and tensile properties of friction stir welded 6061Al joints, *Mater. Sci. Forum* 618–619 (2009) 41–44.
- [27] A.H. Feng, D.L. Chen, Z.Y. Ma, Microstructure and low-cycle fatigue of a friction-stir-welded 6061 aluminum alloy, *Metall. Mater. Trans. A* 41A (2010) 2626–2641.
- [28] G.A. Edwards, K. Stiller, G.L. Dunlop, M.J. Couper, The precipitation sequence in Al–Mg–Si alloys, *Acta Mater.* 46 (1998) 3893–3904.
- [29] A. Simar, Y. Bréchet, B. de Meester, A. Denquin, T. Pardoën, Microstructure, local and global mechanical properties of friction stir welds in aluminium alloy 6005A–T6, *Mater. Sci. Eng. A* 486 (2008) 85–95.
- [30] M.S. Hu, Some effects of particle size on the flow behavior of Al–SiCp composites, *Scripta Metall. Mater.* 25 (1991) 695–700.
- [31] N. Ramakrishnan, An analytical study on strengthening of particulate reinforced metal matrix composites, *Acta Mater.* 44 (1996) 69–77.
- [32] C.W. Nan, D.R. Clarke, The influence of particle size and particle fracture on the elastic/plastic deformation of matrix composites, *Acta Mater.* 44 (1996) 3801–3811.
- [33] W.D. Armstrong, T. Lorentzen, P. Brøndsted, P.H. Larsen, An experimental and modeling investigation of the external strain, internal stress and fiber phase transformation behavior of a NiTi actuated aluminum metal matrix composite, *Acta Mater.* 46 (1998) 3455–3466.
- [34] C.P. Frick, A.M. Ortega, J. Tyber, A.E.M. Maksud, H.J. Maier, Y.N. Liu, K. Gall, Thermal processing of polycrystalline NiTi shape memory alloys, *Mater. Sci. Eng. A* 405 (2005) 34–49.
- [35] J. Khalil-Allafi, A. Dlouhy, G. Eggeler, Ni<sub>4</sub>Ti<sub>3</sub>-precipitation during aging of NiTi shape memory alloys and its influence on martensitic phase transformations, *Acta Mater.* 50 (2002) 4255–4274.